# Lattice Model of a Three-Dimensional Topological Singlet Superconductor with Time-Reversal Symmetry

Andreas P. Schnyder,[1] Shinsei Ryu,[2] and Andreas W. W. Ludwig[3]

[1]*Kavli Institute for Theoretical Physics, University of California, Santa Barbara, California 93106, USA*
[2]*Department of Physics, University of California, Berkeley, California 94720, USA*
[3]*Department of Physics, University of California, Santa Barbara, California 93106, USA*

(Received 16 January 2009; published 15 May 2009)

We study topological phases of time-reversal invariant singlet superconductors in three spatial dimensions. In these systems the topological phases are characterized by an even-numbered winding number $\nu$. At the surface the topological properties of this quantum state manifest themselves through the presence of $\nu$ flavors of gapless Dirac fermion surface states, which are robust against localization from random impurities. We construct a lattice tight-binding model that realizes a topologically nontrivial phase, in which $\nu = \pm 2$. Disorder corresponds to a (nonlocalizing) random SU(2) gauge potential for the surface Dirac fermions, leading to a power-law density of states $\rho(\epsilon) \sim \epsilon^{1/7}$. The bulk effective field theory is proposed to be the (3 + 1)-dimensional SU(2) Yang-Mills theory with a theta term at $\theta = \pi$.

DOI: 10.1103/PhysRevLett.102.196804 PACS numbers: 73.43.−f, 73.20.At, 73.20.Fz, 74.25.Fy

Bloch-Wilson band insulators are commonly believed to be simple and well understood electronic states of matter. However, recent theoretical [1–6] and experimental [7,8] progress has shown that band insulators can exhibit unusual and conducting boundary modes, which are topologically protected, analogous to the edge states of the integer quantum Hall effect (QHE). These so-called $\mathbb{Z}_2$ topological insulators (also known as ''quantum spin Hall'' insulators), which exist in two- and three-dimensional (3D) *time-reversal invariant* (TRI) systems, are characterized by a topological invariant, similar to the Chern number of the integer QHE. Given these newly discovered topological states, one might wonder whether there exists a general organizing principle for topological insulators. Indeed, the integer QHE and the $\mathbb{Z}_2$ topological insulators are in fact part of a larger scheme, discussed in Ref. [6], which provides an exhaustive classification of topological insulators and superconductors (SCs) in terms of spatial dimension and the presence or absence of the two most generic symmetries of the Hamiltonian, time-reversal and particle-hole symmetry [9].

By using this classification scheme, which was originally introduced in the context of disordered systems (Altland-Zirnbauer classification [10]), it was shown in Ref. [6] that, besides the 3D $\mathbb{Z}_2$ topological insulator, there are precisely four more 3D topological quantum states. Among these, there is one which is particularly interesting from the point of view of possible experimental realizations. It is called the topological superconductor (SC) in symmetry class CI in the terminology of Ref. [6] and can be realized in time-reversal invariant singlet BCS SCs. While the bulk is fully gapped in this topological quantum state, there are gapless robust Dirac states at the two-dimensional (2D) boundary. The CI topological SC is unique among 3D topological quantum states in that it does not break SU(2) spin-rotation symmetry (SRS) and therefore supports the transport of spin through gapless surface modes. The different topological phases of the CI topological SC can be characterized by an even-numbered winding number $\nu$, which can be interpreted as the number of species of gapless surface Dirac fermions.

In this Letter, we construct a lattice BCS Hamiltonian which realizes both the topologically trivial and the nontrivial phases of the CI topological SC. We compute the winding number and demonstrate the existence of gapless 2D Dirac fermions at the boundary. The model we consider is defined on the diamond lattice with (the lattice analogue of) *spin singlet d*-wave pairing and has the form of a $4 \times 4$ Bogoliubov–de Gennes (BdG) Hamiltonian. In reciprocal space the noninteracting Hamiltonian reads $H = \sum_{\boldsymbol{k}} \Psi_{\boldsymbol{k}}^\dagger \mathcal{H}(\boldsymbol{k}) \Psi_{\boldsymbol{k}}$, with $\Psi_{\boldsymbol{k}} = (a_{\boldsymbol{k}\uparrow}, b_{\boldsymbol{k}\uparrow}, a_{-\boldsymbol{k}\downarrow}^\dagger, b_{-\boldsymbol{k}\downarrow}^\dagger)^T$, where $a_{\boldsymbol{k},\alpha}$ and $b_{\boldsymbol{k},\alpha}$ represent the electron annihilation operators with spin $\alpha$ and momentum $\boldsymbol{k}$ on sublattice $A$ and $B$ of the diamond lattice, respectively, and

$$\mathcal{H}(\boldsymbol{k}) = \begin{pmatrix} \Theta_{\boldsymbol{k}} & \Phi_{\boldsymbol{k}} & \Delta_{\boldsymbol{k}} & 0 \\ \Phi_{\boldsymbol{k}}^* & -\Theta_{\boldsymbol{k}} & 0 & \Delta_{\boldsymbol{k}} \\ \Delta_{\boldsymbol{k}}^* & 0 & -\Theta_{\boldsymbol{k}} & -\Phi_{-\boldsymbol{k}}^* \\ 0 & \Delta_{\boldsymbol{k}}^* & -\Phi_{-\boldsymbol{k}} & \Theta_{\boldsymbol{k}} \end{pmatrix}. \quad (1)$$

Here the nearest neighbor (NN) hopping term is given by $\Phi_{\boldsymbol{k}} = \sum_{i=1}^4 t_i e^{i\boldsymbol{k}\cdot\boldsymbol{s}_i}$, the next nearest neighbor (NNN) hopping term is $\Theta_{\boldsymbol{k}} = \sum_{i\neq j} t_{ij}' e^{i\boldsymbol{k}\cdot(\boldsymbol{s}_i - \boldsymbol{s}_j)} + \mu_s$, and the pairing potential is $\Delta_{\boldsymbol{k}} = \sum_{i\neq j} \Delta_{ij} e^{i\boldsymbol{k}\cdot(\boldsymbol{s}_i - \boldsymbol{s}_j)}$, where $\boldsymbol{s}_{i=1\ldots4}$ denotes the four first neighbor bond vectors. The NN and NNN hopping amplitudes are parametrized by the vector $t_l$ and the symmetric matrix $t_{ij}'$, respectively. The symmetric matrix $\Delta_{ij}$ denotes the singlet BCS order parameter, and $\mu_s$ is the staggered chemical potential.

From Eq. (1), the energy eigenvalues $E_{\boldsymbol{k}}^{\pm} = \pm\sqrt{|\Phi_{\boldsymbol{k}}|^2 + |\Theta_{\boldsymbol{k}}|^2 + |\Delta_{\boldsymbol{k}}|^2}$ are readily obtained, exhibiting

 

a twofold degeneracy for each $\boldsymbol{k}$. The symmetry operation that realizes particle-hole symmetry (PHS) for a singlet pairing BdG Hamiltonian is given by [6]

$$r_y \mathcal{H}^T(-\boldsymbol{k}) r_y = -\mathcal{H}(\boldsymbol{k}), \tag{2a}$$

where $r_y$ is the second Pauli matrix acting on the particle-hole space. It can be checked that Eq. (1) automatically satisfies symmetry property (2a). If, furthermore, time-reversal symmetry (TRS) is present, $\mathcal{H}(\boldsymbol{k})$ obeys

$$\mathcal{H}^*(-\boldsymbol{k}) = \mathcal{H}(\boldsymbol{k}), \tag{2b}$$

which is the case if the pairing amplitudes $\Delta_{ij}$ are all purely real. The discrete symmetry constraints (2a) and (2b) define the CI symmetry class in the Altland-Zirnbauer classification [6,10]. Note that an arbitrary Hamiltonian belonging to symmetry class CI can be brought into block off-diagonal form. This is achieved by means of a unitary transformation which rotates the $r_\mu$ matrices such that $(r_x, r_y, r_z) \to (r_x, -r_z, r_y)$. Under this rotation $\mathcal{H}(\boldsymbol{k})$ [Eq. (1)] transforms into

$$\mathcal{H}(\boldsymbol{k}) \to \begin{pmatrix} 0 & D(\boldsymbol{k}) \\ D^\dagger(\boldsymbol{k}) & 0 \end{pmatrix}, \tag{3a}$$

where the upper right block is given by

$$D(\boldsymbol{k}) = \begin{pmatrix} \Delta_{\boldsymbol{k}} - i\Theta_{\boldsymbol{k}} & -i\Phi_{\boldsymbol{k}} \\ -i\Phi_{\boldsymbol{k}}^* & \Delta_{\boldsymbol{k}} + i\Theta_{\boldsymbol{k}} \end{pmatrix}, \tag{3b}$$

which satisfies $D^T(-\boldsymbol{k}) = D(\boldsymbol{k})$, since $\Delta_{-\boldsymbol{k}} = \Delta_{\boldsymbol{k}}$ and $\Phi_{-\boldsymbol{k}}^* = \Phi_{\boldsymbol{k}}$.

In order to define a topological invariant for the CI topological insulator, we need to introduce, following Ref. [6], the projection operator $Q(\boldsymbol{k})$

$$Q(\boldsymbol{k}) = \begin{pmatrix} 0 & q(\boldsymbol{k}) \\ q^\dagger(\boldsymbol{k}) & 0 \end{pmatrix}, \qquad q(\boldsymbol{k}) = \frac{-D(\boldsymbol{k})}{E^+(\boldsymbol{k})}, \tag{4}$$

where, as a consequence of TRI and PHS, $q^T(-\boldsymbol{k}) = q(\boldsymbol{k})$. The block off-diagonal form of $\mathcal{H}(\boldsymbol{k})$, and hence of $Q(\boldsymbol{k})$, is essential to uncover the topological structure of the space of all possible quantum ground states in class CI. It allows us to introduce a topological invariant that classifies maps from the Brillouin zone (BZ) into the space of the projection operators $Q(\boldsymbol{k})$. This invariant is a winding number defined in Ref. [6] through

$$\nu[q] = \int \frac{d^3\boldsymbol{k}}{24\pi^2} \epsilon^{\mu\nu\rho} \,\mathrm{tr}[(q^{-1}\partial_\mu q)(q^{-1}\partial_\nu q)(q^{-1}\partial_\rho q)], \tag{5}$$

where the integral is over the 3D BZ [11]. Because of the class CI constraint $q^T(-\boldsymbol{k}) = q(\boldsymbol{k})$, $\nu$ can take on only even integer values. The winding number changes only when the quantum system undergoes a quantum phase transition, which is accompanied by the closing of the bulk gap.

We now turn to a more detailed specification of our lattice model. When $t_l = t$ for all $l = 1, \ldots, 4$, one has

$$\Phi_{\boldsymbol{k}} = 2t\left[e^{+i(k_z/4)} \cos\frac{k_x + k_y}{4} + e^{-i(k_z/4)} \cos\frac{k_x - k_y}{4}\right]. \tag{6}$$

We consider a $d$-wave pairing potential, where the pairing amplitude on bonds within the $x$-$y$ plane differs in sign from the out-of-plane pairing amplitudes [see Fig. 1(a)]:

$$\Delta_{\boldsymbol{k}} = 4\Delta\left[\cos\frac{k_x}{2}\cos\frac{k_y}{2} - \cos\frac{k_y}{2}\cos\frac{k_z}{2} - \cos\frac{k_z}{2}\cos\frac{k_x}{2}\right]. \tag{7}$$

For definitiveness we will take $t$ and $\Delta$ positive throughout this Letter. The BCS dispersion given by $\Phi_{\boldsymbol{k}}$ and $\Delta_{\boldsymbol{k}}$ has four point nodes (Dirac points), at which the bands are fourfold degenerate $K_{1,\pm} = 2\pi(\pm 1/3,\ 1,\ 0)$ and $K_{2,\pm} = 2\pi(1,\ \pm 1/3,\ 0)$. Note that PHS and TRI relate $K_{a,+}$ to $K_{a,-}$ $(a = 1, 2)$, as $K_{a,-}$ is identified to $-K_{a,+}$ via a translation by reciprocal lattice vectors. The degeneracy at the point nodes can be lifted by a finite staggered sublattice potential or by NNN hopping amplitudes, which are parametrized by the symmetric matrix $t'_{ij}$. In order to open up a bulk gap, we choose $t'_{13} = -t'_{14} = +t'_{24} = -t'_{23} \equiv t' \neq 0$, while $t'_{12} = t'_{34} = 0$, in which case the NNN hopping term simplifies to [see Fig. 1(a)]

$$\Theta_{\boldsymbol{k}} = 4t' \cos\frac{k_z}{2}\left(\cos\frac{k_y}{2} - \cos\frac{k_x}{2}\right) + \mu_s, \tag{8}$$

where we also include a staggered chemical potential.

The BdG Hamiltonian (1) has four energy bands, two of which are occupied. With the choice for the hopping parameters and gap amplitudes given by Eqs. (6)–(8), the spectrum has a bulk energy gap, except when $\pm 6t' = \mu_s$, i.e., when the system undergoes a quantum phase transition between different topological phases. The winding number $\nu$ [Eq. (5)] for this model can be computed numerically, by discretizing the integral over the BZ [see Fig. 2(b)]. With an increasing number of grid points in the BZ, the integral (5) converges rapidly to an even integer value. In this way we obtain the phase diagram shown in Fig. 2(a), which contains four distinct gapped phases. The nontrivial phases $(\nu = \pm 2)$ occur if $|\mu_s| < |6t'|$. Inclusion of finite (but small) NNN terms $t'_{12}$ and $t'_{34}$ shifts the phase boundaries but does not change the topology of the phase diagram.

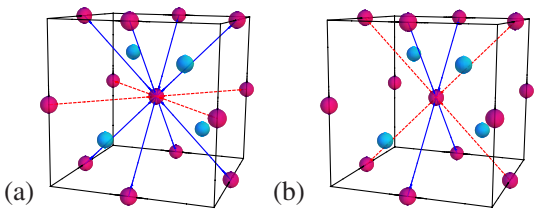


FIG. 1 (color online). The diamond lattice has two sublattices colored in blue (light) and red (dark), respectively. (a) The pairing amplitude and (b) the second neighbor hopping are schematically shown, where the red dashed bonds and the blue solid bonds have pairing potentials or second neighbor hopping amplitudes which differ by a sign.

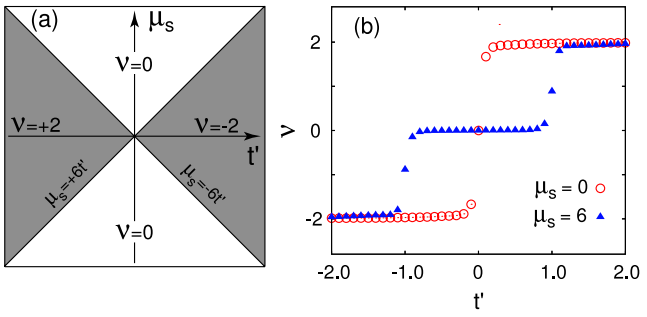


FIG. 2 (color online). (a) Phase diagram as a function of NNN hopping $t'$ and staggered chemical potential $\mu_s$. (b) Numerical evaluation of the winding number $\nu$ with $t = 4$ and $\Delta = 2$.

When $\mu_s$ and $t'$ are small compared to $t$ [see Fig. 2(a)], an effective low-energy continuum description can be derived by expanding Eq. (3) around the four nodal points $K_{1/2,\pm}$. Rescaling momenta as $tk_z/2 \to k_z$, $t\sqrt{3}k_y/2 \to k_y$, and $2\sqrt{3}\Delta k_x \to k_x$ and performing a unitary transformation, we find that the expansion around the node $K_{1\pm}$ of the off-diagonal block in Eq. (3a) is given by

$$D(\boldsymbol{q}) = \beta i\sigma_y[\tilde{\boldsymbol{q}} \cdot \boldsymbol{\alpha} - i(\mu_s + 6t')\gamma^5], \tag{9}$$

where $\tilde{\boldsymbol{q}} = (q_x, -q_y, -q_z)$ denotes the deviation of the momentum from $K_{1\pm}$. Equation (9) is identical to the class CI topological Dirac SC constructed in Ref. [6]. Here we have introduced the five gamma matrices $\alpha_\mu$, $\beta$, and $\gamma^5$, which are in the Dirac representation given by $\alpha_\mu = \sigma_\mu \otimes \tau_x$, $\beta = \tau_z$, and $\gamma^5 = \tau_x$, with $\tau_{x,y,z}$ being another set of Pauli matrices. Consequently, the winding number within the continuum description for the nodes $K_{1,\pm}$ is

$$\nu_1 = \frac{1}{2}\frac{(\mu_s + 6t')}{|\mu_s + 6t'|} \times 2, \tag{10}$$

where the prefactor $1/2$, which is an artifact of the low-energy continuum approximation, will be altered once information about the structure of Bloch wave functions at high energy (located away from the Dirac points) is supplemented. The low-energy Dirac Hamiltonian for the nodes $K_{2,\pm}$ is related by symmetry to the result for the nodes $K_{1\pm}$ by simultaneously interchanging $k_x$ with $k_y$ and replacing the mass term $\mu_s + 6t'$ with $\mu_s - 6t'$:

$$D(\boldsymbol{q}) = \beta i\sigma_y[\tilde{\boldsymbol{q}} \cdot \boldsymbol{\alpha} - i(\mu_s - 6t')\gamma^5], \tag{11}$$

where $\tilde{\boldsymbol{q}} = (q_y, -q_x, -q_z)$. Similarly, the winding number within the continuum description for the nodes $K_{2,\pm}$ is

$$\nu_2 = -\frac{1}{2}\frac{(\mu_s - 6t')}{|\mu_s - 6t'|} \times 2. \tag{12}$$

Interestingly, the winding number obtained from the continuum description, $\nu = \nu_1 + \nu_2$, reproduces the phase diagram of the lattice model correctly.

A physical consequence of the nonzero winding number $\nu$ is the appearance of zero-energy surface Andreev bound states with Dirac dispersion. To study these surface states, we solve model (1) in a slab geometry and compute the energy bands for a slab parallel to the (111) surface. As shown in Fig. 3, where we set $t = 4$ and $\Delta = 2$, there are, in addition to the bulk states, surface Dirac states which cross the band gap. When the bulk topological invariant is $\nu = 2$ [Fig. 3(c)], there are two surface Dirac states, whereas there is no such state when the bulk topological invariant is $\nu = 0$ [Fig. 3(d)]. Hence, the total number of Dirac cones $N_f = 2$ is consistent with the bulk characteristics $\nu = 2$. $N_f = 2$ is the minimal number of Dirac cones required by class CI symmetries. Note, however, that in any 2D lattice model satisfying the CI symmetries, the possible number of Dirac cones is an integer multiple of $2N_f$ because of a no-go theorem analogous to the fermion doubling theorem of Ref. [12]. Here the fermion doubling is avoided since the 2D system is realized as a boundary of a 3D bulk.

The surface Dirac fermion modes cannot be gapped by any deformation of the Hamiltonian respecting TRS and PHS. Indeed, this is so because any perturbation respecting the class CI symmetries takes the form of an SU(2) gauge field (see Ref. [6]), which perturbs the surface Dirac fermions in the following way:

$$\mathcal{H} = (k_x + \boldsymbol{a}_x \cdot \boldsymbol{\sigma})\tau_x + (k_x + \boldsymbol{a}_y \cdot \boldsymbol{\sigma})\tau_y, \tag{13}$$

where $a^{a=1,2,3}_{\mu=x,y} \in \mathbb{R}$. The gapless nature of this four-component Dirac fermion is stable against arbitrary values of the six real parameters $a^a_\mu$; i.e., the non-Abelian gauge potential shifts the location of the Dirac node but does not lead to a gap. With the inclusion of randomness, small

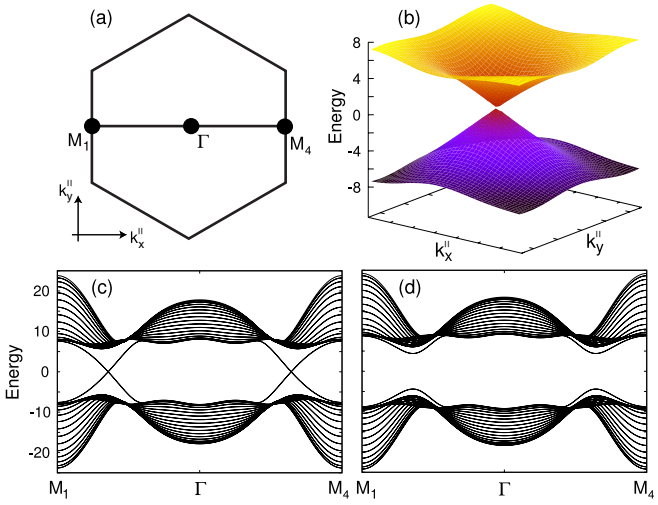


FIG. 3 (color online). (a) Surface BZ for a slab parallel to the (111) surface. (c) and (d) show the 2D band structure for the model defined by Eqs. (1) and (6)–(8) terminated by a (111) surface, with the momentum being varied along the line indicated in (a). For $(t', \mu) = (1.2, 0)$ [(c)] there are surface states which cross the bulk energy gap, thereby realizing a surface Dirac fermion state as shown in (b). In the trivial phase, for $(t', \mu) = (0, 4.4)$ [(d)], there are no surface states crossing the energy gap.

relative to the bulk energy gap, the surface Dirac fermion mode realizes the random SU(2) gauge potential model discussed in Ref. [13]. The random SU(2) gauge potential, known not to be able to localize the Dirac fermions, renormalizes to an exactly solved strong coupling renormalization group fixed point at long distances, without modifying the surface conductivity. With disorder, the (tunneling) density of states $\rho(\epsilon)$ changes from a linear dependence to $\rho(\epsilon) \sim |\epsilon|^{\mu}$, with the scaling exponent $\mu = 1/7$ [13] at this fixed point.

Within the replica nonlinear sigma model approach (based on $n$ fermionic replicas $n \to 0$) the Anderson localization physics at the surface of the 3D class CI topological SC in the presence of disorder is described by the principal chiral model on Sp($2n$), supplemented by a Wess-Zumino-Witten (WZW) term, at ''level one.'' [When supersymmetric disorder averaging is used, this is [14] the WZW model on Osp(2|2) at level $-\nu$ [15].] We emphasize that the WZW term cannot appear for any 2D disordered systems on a lattice, as the WZW terms always turn out to cancel when contributions from different cones are added up.

As it stands, the lattice model we considered is presumably not directly connected to any specific system occurring in nature, but it may give insight into the properties of real materials that exhibit 3D topological phases which preserve both TRS and SRS. Candidates for the CI topological quantum state might be found among some of the unconventional SCs of heavy fermion systems. There are various ways how the topologically protected surface states in such compounds could be detected experimentally. First of all, the surface conductivity for the spin current or for the thermal current is unchanged by symmetry preserving perturbations, including disorder. Second, the density of states of the surface states can be probed via tunneling experiments. Finally, we argue that by breaking TRS locally at the surface, while keeping the SRS intact, one can realize the so-called ''*spin quantum Hall effect*'' (SQHE) [16] in symmetry class C (unrelated to the ''quantum spin Hall insulators'' mentioned earlier) at the surface of the CI topological SC. Indeed, broken TRS [without breaking SU(2) symmetry] allows for the appearance of four additional perturbing potentials in Eq. (13), describing the surface modes. One can check that only one of theses additional potentials gives rise to a gap and hence to a (2D) nonzero Chern integer $n = \pm 1$; this is one-half of the allowed value of the Chern number in any 2D system exhibiting the SQHE [16]. This situation is completely analogous to the half-integer surface QHE of the 3D $\mathbb{Z}_2$ topological insulator [4,17,18].

In the 3D $\mathbb{Z}_2$ topological insulator, this topological magnetoelectric effect can be described by the effective field theory whose action is given by (3 + 1) QED supplemented with a $\theta = \pi$ term [17,18]. Since spin is a good quantum number in a singlet SC, it is possible to describe its spin transport in terms of an external SU(2) gauge field. Indeed, the effective field theory of the SQHE in TRS-breaking 2D singlet SCs is known to be the SU(2) Chern-Simons theory at an integer level [19]. Then, following the same reasoning as in the case of the 3D $\mathbb{Z}_2$ topological insulators, we propose that the effective field theory describing class CI topological SC is the (3 + 1)D SU(2) Yang-Mills theory augmented with the theta term $\mathcal{L} = \theta/(32\pi^2)\epsilon^{\mu\nu\kappa\lambda}\,\mathrm{tr}(F_{\mu\nu}F_{\kappa\lambda})$, where $F_{\mu\nu}$ is the SU(2) field strength and $\theta = \pi$.

We are grateful to the KITP and all participants of the quantum spin Hall program. This work is supported in part by NSF Grants No. PHY05-51164 (S. R. and A. S.) and No. DMR-0706140 (A. W. W. L.). S. R. thanks the Center for Condensed Matter Theory at UCB for its support.

[1] C. L. Kane and E. J. Mele, Phys. Rev. Lett. **95**, 146802 (2005); **95**, 226801 (2005).
[2] B. A. Bernevig, T. L. Hughes, and S.-C. Zhang, Science **314**, 1757 (2006).
[3] J. E. Moore and L. Balents, Phys. Rev. B **75**, 121306(R) (2007).
[4] L. Fu, C. L. Kane, and E. J. Mele, Phys. Rev. Lett. **98**, 106803 (2007).
[5] L. Fu and C. L. Kane, Phys. Rev. B **76**, 045302 (2007).
[6] A. P. Schnyder *et al.*, Phys. Rev. B **78**, 195125 (2008); AIP Conf. Proc. **1134**, 10 (2009); arXiv:0905.2029; see also http://landau100.itp.ac.ru/Talks/ludwig.pdf.
[7] M. König *et al.*, Science **318**, 766 (2007).
[8] D. Hsieh *et al.*, Nature (London) **452**, 970 (2008).
[9] The same conclusion has recently been reached from $K$ theory by A. Yu. Kitaev, AIP Conf. Proc. **1134**, 22 (2009); see also arXiv:0901.2686.
[10] M. R. Zirnbauer, J. Math. Phys. (N.Y.) **37**, 4986 (1996); A. Altland and M. R. Zirnbauer, Phys. Rev. B **55**, 1142 (1997); P. Heinzner, A. Huck Leberry, and M. R. Zirnbauer, Commun. Math. Phys. **257**, 725 (2005).
[11] A topological invariant of a similar type was discussed in the context of the B phase in $^3$He by M. M. Salomaa and G. E. Volovik, Phys. Rev. B **37**, 9298 (1988).
[12] H. B. Nielsen and M. Ninomiya, Nucl. Phys. **B185**, 20 (1981).
[13] A. M. Tsvelik, Phys. Rev. B **51**, 9449 (1995).
[14] M. J. Bhaseen *et al.*, Nucl. Phys. **B618**, 465 (2001); A. W. W. Ludwig, arXiv:cond-mat/0012189.
[15] More generally, on surfaces of 3D topological insulators in classes AIII and DIII of Ref. [6], the WZW model on $\mathrm{Gl}(1|1)_{\nu}$ and $\mathrm{Osp}(2|2)_{\nu}$, respectively, appears in the presence of disorder, where $\nu$ is the topological winding number in the bulk. See Ref. [6] and, e.g., A. LeClair and D. J. Robinson, J. Phys. A **41**, 452002 (2008).
[16] T. Senthil, J. B. Marston, and M. P. A. Fisher, Phys. Rev. B **60**, 4245 (1999); I. A. Gruzberg, A. W. W. Ludwig, and N. Read, Phys. Rev. Lett. **82**, 4524 (1999).
[17] X.-L. Qi, T. Hughes, and S.-C. Zhang, Phys. Rev. B **78**, 195424 (2008).
[18] A. M. Essin, J. E. Moore, and D. Vanderbilt, Phys. Rev. Lett. **102**, 146805 (2009).
[19] N. Read and D. Green, Phys. Rev. B **61**, 10 267 (2000).